Conformation and Protonation of 2,2′-Bipyridine and 4,4′-Bipyridine in Acidic Aqueous Media and Acidic ZSM-5 Zeolites: A Raman Scattering Study

Alain Moissette,* Yann Batonneau, and Claude Brémard

Contribution from the Laboratoire de Spectrochimie Infrarouge et Raman UMR-CNRS 8516, Centre d'Etudes et de Recherches Lasers et Applications, Bât. C5 Université des Sciences et Technologies de Lille, 59655 Villeneuve d'Ascq Cedex, France

Received July 23, 2001

Abstract: In situ FT-Raman scattering spectroscopy was used to monitor the sorption kinetics of 2,2′- and 4,4′-bipyridine in acidic ZSM-5 zeolites. The data processing of all the Raman spectra was applied to extract the characteristic Raman spectra of occluded species and respective Raman contribution generated from many spectral data which resolves spectrum of mixture into pure component spectra without any prior information. The assignment of the extracted spectra was performed according to careful comparison with corresponding spectra extracted from a set of Raman spectra recorded during the protonation of 2,2′- or 4,4′-bipyridine (bpy) in hydrochloric acid aqueous solutions. The data processing of the Raman spectra recorded during the slow sorption of 4,4′-bpy in acidic H_nZSM-5 ($n = 3, 6$) zeolites provides specific Raman spectrum of N,N′-diprotonated dication 4,4′-bpyH_2^{2+} as unique species generated in the void space of acidic ZSM-5 zeolites. No evidence of Lewis acid sites was found during the sorption of 4,4′-bpy by Raman scattering spectroscopy. The data processing of the Raman spectra recorded during the slow sorption of 2,2′-bpy in acidic H_nZSM-5 ($n = 3, 6$) zeolites provides specific Raman spectrum of *trans*-N-monoprotonated cation 2,2′-bpyH^+ as major species generated in the void space of acidic ZSM-5 zeolites at loading corresponding to 1 mol per unit cell. The *trans/cis* interconversion occurs at higher loading even after the complete uptake of the sorbate and indicates some rearrangement in the void space over a long time. The cations were found to be located in straight channels in the vicinity of the intersection with the zigzag channel of the porous materials with the expected conformations deduced from ab initio calculations. However, the motions of occluded species within the channel of ZSM-5 are hindered but remain in the range of the isotropic limit of a liquid at room temperature.

Introduction

Aromatic nitrogen-containing heterocycles including pyridine represent an important class of molecules implicated in several applications including storage energy and catalytic oxidation.[1−3] The 2,2′-bipyridine and 4,4′-bipyridine abbreviated hereafter 2,2′-bpy and 4,4′-bpy, respectively, have been extensively investigated, with respect to their ability as electron acceptors, electron carriers, proton sponges, and chelating agents.[1,4,5] In 2,2′-bipyridine and 4,4′-bipyridine, two planar pyridine rings are connected via a C−C bond. The influence of the rotation of the pyridyl rings around the central C−C bond on the basicity or proton affinity is expected from theoretical works.[4,6] Recently, unusual conformations of 2,2′-bpy and 4,4′-bpy were found to be stabilized in the porous void of non-acidic-MFI zeolites [$M_n(AlO_2)_n(SiO_2)_{96-n}$; M = Na^+, Zn^{2+}; $n = 0, 3, 6$].[7,8] In addition, the adsorption of bipyridines on gold surfaces in aqueous media was reported to depend on both the conformation and proton affinity.[9,10] Despite the large volume of literature devoted to 2,2′-bpy, there are no detailed reports on vibrational spectra in aqueous media to characterize both the conformation and proton affinity.[11] Pyridine is often used as a probe molecule in vibrational spectroscopic studies to characterize Brønsted (protonic) and Lewis (electron acceptor) acid sites in catalytic materials such as zeolites.[12] In particular, H-ZSM-5 zeolite has attracted much attention because of its interesting catalytic properties including shape, selectivity, and high acid strength.[13] Pyridine molecule is rather bulky; the so-called kinetic diameter of the flat-shaped molecule is about 0.6 nm. Pyridine is suitable for probing medium-pore structures such as ZSM-5, ZSM-11, silicalite (10-membered ring opening ≈ 0.6 nm diameter). However, the diffusivities of pyridine in such porous systems were found to be low. The rod-shaped bpy molecules can penetrate within the porous void space of ZSM-5 zeolites. However, the sorption of 2,2′-bpy or 4,4′-bpy in H_nZSM-5 is expected to be very slow.[7,8]

In this article, we present (i) the study of protonation of 2,2′-bpy and 4,4′-bpy in aqueous media by Raman scattering and

(1) Gratzel, M. Acc. *Chem. Res.* **1981**, *14*, 376.
(2) Vitale, M.; Castagnola, N. B.; Ortins, N. J.; Brooke, J. A.; Vaidyalingam, A.; Dutta, P. K. *J. Phys. Chem. B* **1999**, *103*, 2408.
(3) Knops-Gerrits, P. P.; De Vos, D.; Thibault- Starzyk, F.; Jacobs, P. A. *Nature* **1994**, *369* (6481), 543.
(4) Howard, S. T. *J. Am. Chem. Soc.* **1996**, *118*, 10269.
(5) Steel, P. *Coord. Chem. Rev.* **1990**, *106*, 227.
(6) Raczynska, E. D. *THEOCHEM* **1990**, *427*, 87.
(7) Moissette, A.; Gener, I.; Brémard, C. *J. Phys. Chem. B* **2001**, *105*, 5647.
(8) Moissette, A.; Brémard, C. *Microporous Mesoporous Mater.* **2001**, *47*, 345.
(9) Futamata, M. *Chem. Phys. Lett.* **2000**, *332*, 421.
(10) Dretschkow, T.; Lampner, D.; Wandlowski, T. *J. Electroanal. Chem.* **1998**, *458*, 121.
(11) Kaes, C.; Katz, A.; Hosseini, M. W. *Chem. Rev.* **2000**, *100*, 3553.
(12) Knözinger, H. *Adv. Catal.* **1976**, *25*, 184.
(13) Bludau, H.; Karge, H. G.; Niessen, W. *Microporous Mesoporous Mater.* **1998**, *22*, 297.

10.1021/ja011787b CCC: $20.00
Published on Web 11/10/2001

data processing and (ii) the results of spectroscopic investigations of the sorption of 2,2′-bpy and 4,4′-bpy in acidic H_nZSM-5 zeolites. The steric, electrostatic constraints and Brønsted acidity strength of the porous materials on the conformational change ability and protonation of 2,2′-bpy and 4,4′-bpy are compared with solvent effects of acidic aqueous solutions through the respective Raman spectrum and concentration of protonated species.

Experimental Section

Materials. The NH_4^+-exchanged ZSM-5 samples (Si/Al = 13, 27, particle size 2 μm) were obtained from VAW aluminum (Schwandorf, Germany). A ZSM-5 zeolite sample (Si/Al = 31, particle size 5 μm) was synthesized in high purity according to the fluoride medium procedure and was a gift of Dr J. Patarin (Laboratoire des Matériaux Minéraux, ESA 7016, CNRS-ENSC Mulhouse). All the zeolite samples were used after a calcination procedure under air or argon at 773 K. The unit cell composition of the calcined H_nZSM-5 samples were found to be $H_{3.0}(AlO_2)_{3.0}(SiO_2)_{93.0}$ (Si/Al = 31); $H_{3.4}(AlO_2)_{3.4}(SiO_2)_{92.6}$ (Si/Al = 27) and $H_{6.6}(AlO_2)_{6.6}(SiO_2)_{89.4}$ (Si/Al = 13) from elemental analysis. The 2,2′-bipyridine and 4,4′-bipyridine ($C_{10}H_8N_2$, Merck), were used after bisublimation procedure. Aqueous solutions of hydrochloric acid were obtained from high purity concentrated HCl (36%, SIGMA) and deionized and deaerated water. Pure and dry Ar and O_2 gas were used.

Protonation of 2,2′- and 4,4′-bpy in Aqueous Media. Weighted amounts of bpy ($C_{10}H_8N_2$) were dissolved in hydrochloric acid aqueous solutions to obtain homogeneous solutions with $\sim 5 \times 10^{-2}$ mol·L^{-1} concentration in acidic media in the 10^{-3} to 12 N range. In very acidic (1−12 N) media, the bpy solubility permits to obtain homogeneous solution with 0.3 mol·L^{-1} concentration. The solutions were then transferred in quartz glass Suprasil cuvettes for FT-Raman and UV−visible experiments, respectively.

Sorption of 2,2′- and 4,4′-bpy in Acidic ZSM-5. Weighted amounts ($\sim$1.4 g) of powdered hydrated zeolite $H_n(AlO_2)_n(SiO_2)_{96-n}$ were introduced into an evacuable heatable silica cell. The sample was dried under vacuum (10^{-3} Pa) and heated stepwise to 773 K under O_2 or Ar. The thermal treatment removed completely the water content. The crystallinity of the samples was checked by XRD and was not reduced by this treatment. Then, the sample was held under vacuum and cooled to room temperature under dry argon. Weighted amounts of bpy corresponding to 1 or 2 bpy per unit cell (UC) were introduced into the cell under dry Ar and the powder mixture was shaken. The sample was transferred under dry argon in a quartz glass Suprasil cuvette for FT-Raman and diffuse reflectance UV−visible experiments. The cuvette tubes were sealed under argon or under vacuum. All the spectra recorded with two types of sampling were found to be analogous. The cuvettes were kept in the dark at room temperature. Bulk solid bpy stocked in these conditions exhibits no change in the Raman and UV−visible spectra over at least one year.

Instrumentation. The elemental analyses (C, H, Al, Si) of the bare and loaded zeolites were obtained from the Service Central d'Analyse du Centre National de la Recherche Scientifique (Vernaison, France).

X-ray powder diffractograms were obtained using a Siemens D-5000 X-ray diffractometer with Cu Kα radiation.

The ^{27}Al magic angle spinning nuclear magnetic resonance (MAS NMR) measurements were performed on a Bruker MSL-400 spectrometer with a magnetic field strength of 9.4 T and a resonance frequency of 104.26 MHz. The spectra were recorded with 0.1 s delay time, a pulse length of 0.6 μs, and a magic angle spinning frequency of 12 kHz. A 0.5 M $Al(NO_3)_3$ solution was used as a reference.

The UV−visible absorption spectra of the sample were recorded between 200 and 800 nm using a Cary 3 spectrometer. The instrument was equipped with an integrating sphere to study the powdered zeolite samples through diffuse reflectance; the corresponding bare zeolite was used as the reference.

A Bruker IFS 88 instrument was used as a near-IR FT-Raman spectrometer with a cw Nd:YAG laser at 1064 nm as excitation source. A laser power of 100−200 mW was used. The spectra (3500−150 cm^{-1}) were recorded with 2 cm^{-1} resolution using 600 scans. The Opus Bruker software was used for spectral acquisition, data treatment and plotting. Data analysis were performed on a PC, AMDAthlon1.3 GHz, 768 MB of RAM, running Microsoft Windows version 2000 professional, and using SIMPLISMA programs. All SIMPLISMA algorithms were implemented in MATLAB Version 6.0 software package (MathWorks Inc., Matick, MA).

The FTIR spectrometer was a Bruker IFS 113V instrument equipped with a liquid nitrogen cooled MCT detector (mid-IR) with the suitable beam splitter. The spectra were recorded with 2 cm^{-1} resolution. The in situ diffuse reflectance apparatus is a Harrick scientific diffused reflectance attachment "DRA-2CI" Praying mantis and "HVC-DRP" cell equipped with CaF_2 windows.

The structural modeling calculations were performed on a Silicon Graphics workstation using Cerius^2 (version 3.8) package from Molecular Simulations.

Self-Modeling Mixture Analysis. The data processing of all the Raman spectra recorded after the acid addition or during the course of the sorption was performed using the SIMPLISMA (SIMPLe-to-use Interactive Self-modeling Mixture Analysis) approach.[14,15]

This method was applied to extract the characteristic Raman spectra of species and respective concentration generated from many spectral data which resolves spectrum of mixture into pure component spectra without any prior information. The mathematical principle of SIMPLISMA lies in the presence of pure variable. A pure variable (wavenumber for Raman spectra) is hypothetically a variable that has an intensity contribution from only one of the mixture components. Such a requirement is not automatically met for each data set under study. In such cases, they are instead better named key variable.[16] When such situations occur, the possibility to resolve the data property by using second derivative spectra as an intermediate step has been shown.[17,18] Therefore, once the experimental spectra have been twice derived, the sign of the so-called "2nd derivative" spectra is changed to obtain positive peaks at the same wavenumber as that of the original spectra. As a consequence, the operation was referred to as inverted second-derivative spectra. The obtained spectra still have negative parts, which is very problematic for the pure variable approach which inherently requires positive spectra. Previous works dealing with this problem showed the validity of setting the negative values of the transformed spectra to zero. That implies in the present work an almost complete overlap elimination of the overlapped Raman peaks.

The pure variable intensities can be used as a concentration estimate in the following relation.

$$D = CP^{\mathrm{T}} \tag{1}$$

D represents the original data matrix with the spectra in rows, C represents the "concentration" matrix, obtained by using the columns of C that represent pure variables. P (respectively, P^{T}) represents the matrix (respectively the transpose of the matrix) with the spectra of the pure components in its columns. Typically, D exists, but C and P are not known. When the matrices D and C are known (C becomes known through the pure variable selection in the SIMPLISMA algorithm) P can be calculated by standard matrix algebra.

$$P = D^{\mathrm{T}}C(C^{\mathrm{T}}C)^{-1} \tag{2}$$

In a next step, the contributions are now calculated from P, which are basically a projection of the original pure variable intensities in the original data set. This step reduces the noise in the contributions. The equation is

$$C^* = DP(P^{\mathrm{T}}P)^{-1} \tag{3}$$

where C^* stands for the projected C. Because matrix C does not contain concentrations but intensities proportional to concentrations, scaling procedures such as normalization of the resulting spectra in P and the

(14) Windig, W.; Guilment, J. *Anal. Chem.* **1991**, *63*, 1425.
(15) Windig, W. *Chemom. Intell. Lab. Syst.* **1997**, *36*, 3.
(16) Schostack, K. J.; Malinowski, E. R. *Chemom. Intell. Lab. Syst.* **1989**, *6*, 21.
(17) Windig, W.; Stephenson, D. A. *Anal. Chem.* **1992**, *64*, 2735.
(18) Windig, W. *Chemom. Intell. Lab. Syst.* **1994**, *23*, 71.

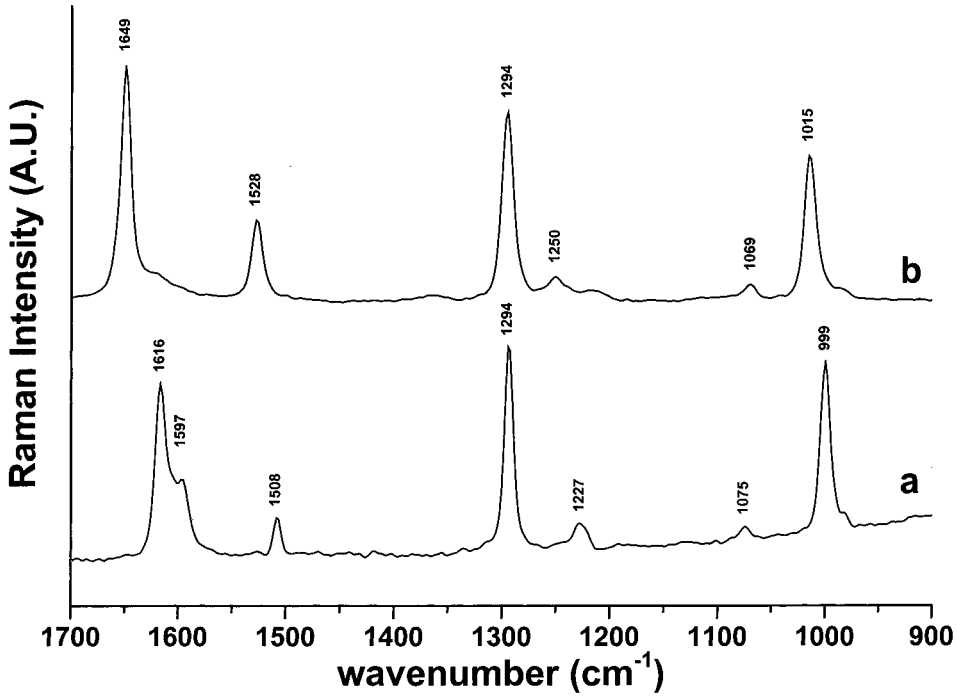

Figure 1. Raman spectra of 4,4′-bpy and 4,4′-bpyH_2^{2+} recorded in aqueous solutions by FT-Raman spectrometry at room temperature in the mid frequency region: (a) 4,4′-bpy, pH = 9; (b) 4,4′-bpyH_2^{2+}, pH = 0.

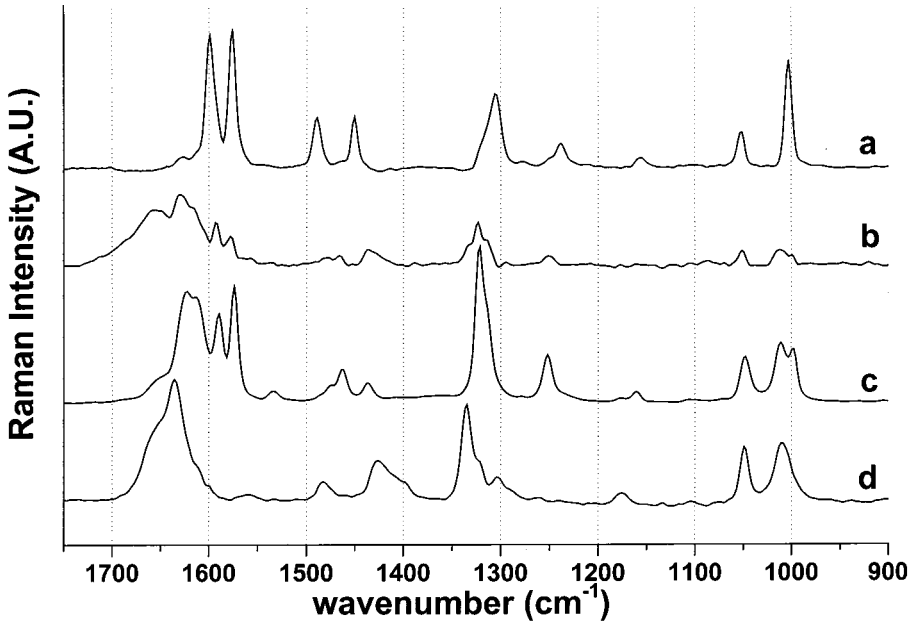

Figure 2. Pure Raman spectra extracted by the SIMPLISMA method of the FT-Raman data recorded during the protonation of 2,2′-bpy in hydrochloric acid solutions: (a) *trans*-2,2′-bpy; (b) *trans*-2,2′-bpyH^+; (c) *cis*-2,2′-bpyH^+; (d) 2,2′-bpyH_2^{2+}.

associated inverse normalization of C are often used to obtain the relative contributions of the components. The data set can be reconstructed as follows:

$$D^{\text{reconstructed}} = C^{*}P^{\text{T}} \tag{4}$$

The relative root sum of squares (RRSSQ) coefficient calculates residuals and represents the difference between the reconstructed and the original data. This coefficient can be seen as a standard deviation and was defined previously.[14,15] The values are between 0 and 1.

The algorithm for pure variables in SIMPLISMA is described in detail elsewhere.[14,15]

The Model: Structure, Force Field, Calculations. The atomic positions for the zeolite framework H-ZSM-5 were obtained from previous X-ray determinations of the MFI structures.[19−21] For computer calculations, the simulation box consists of two crystallographic cells superimposed along the *c* direction. The partial atomic charges of the zeolite atoms were taken from previous work; ZSM-5: Si = +1.56, Al = +1.232, O = −0.794, H = +1.[7] The geometrical parameters of $bpyH_n^{n+}$ and the partial atomic charges were derived from previous ab initio calculations and X-ray determination.[4,22]

The potential energy $\boldsymbol{E}$ of the simulated zeolite−sorbate (**Z**−**S**) system is generally calculated by the summation of four terms: the bonded interaction energy of **Z**, $\boldsymbol{E}_{\mathbf{Z}}$; the bonded interaction energy of **S**, $\boldsymbol{E}_{\mathbf{S}}$; the nonbonded interaction energy between **Z** and **S**, $\boldsymbol{E}_{\mathbf{ZS}}$; the

(19) Van Koningsveld, H.; Jansen, J. C.; van Bekkum, H. *Zeolites* **1990**, *10*, 235.
(20) Van Koningsveld, H. *Acta Crystallogr*. **1990**, *B46*, 731.
(21) Van Koningsveld, H.; Van Bekkum, H.; Jansen, J. C. *Acta Crystallogr*. **1987**, *43 B*, 127.
(22) Castella-Ventura, M.; Kassab, E. *J. Raman Spectrosc*. **1998**, *29*, 511.

Table 1: Raman Wavenumbers (cm^{-1}) for Protonated 2,2′-Bipyridine in HCl Solution and Occluded in HZSM-5 Zeolite

solution			occluded		tentative assignment[a]
2,2′-bpyH$_2^{2+}$	*trans*-2,2′-bpyH$^+$	*cis*-2,2′-bpyH$^+$	*trans*-2,2′-bpyH$^+$	*cis*-2,2′-bpyH$^+$	[28]
∼3110	∼3110	∼3110	∼3110	∼3110	NH stretch
∼3070	∼3070	∼3070	∼3070	∼3070	CH stretch
1655 (sh.)	1655		1655		ring stretch
1636	1628	1622	1628	1628	
	1614	1614	1612	1613	
	1591	1589	1585	1587	ring stretch
1560 (w)	1578	1574	1572	1572	ring stretch
		1531		1535	
1481	1466	1462	1468	1462	CH i.p. bend + ring stretch
1426	1437	1437	1429	1437	CH i.p. bend
1402 (sh.)					
1335	1323	1321	1319	1317	CH bend
1302					
	1250	1252	1248	1248	ring stretch
1175	1176	1159	1173	1157	CH i.p. bend
1050	1051	1048	1048	1048	ring stretch + ring i.p. def.
1010	1013	1011	1017	1018	ring i.p. deformation
	999	997	999	997	ring i.p. deformation

[a] i.p.: in plane; o.p.: out of plane; sh.: shoulder; w: weak.

nonbonded interaction energy between **S** and **S**, $\boldsymbol{E}_{\mathbf{SS}}$. The force field values (bond, angle, torsion) to calculate the $\boldsymbol{E}_{\mathbf{Z}}$ term were derived from ab initio calculations of small model systems. The force field values to calculate the $\boldsymbol{E}_{\mathbf{S}}$, $\boldsymbol{E}_{\mathbf{ZS}}$, and $\boldsymbol{E}_{\mathbf{SS}}$ terms were derived from previous works. All the details of the force field and calculation were given in a recent work.[7]

The sum of a Coulombic potential and a Lennard-Jones (L−J) potential is used to describe the nonbonded interactions.

$$E_{ZS} = \sum_{ij} A_{\alpha\beta}/r_{ij}^{12} - B_{\alpha\beta}/r_{ij}^{6} + q_i q_j / r_{ij} \qquad (5)$$

The L−J potential accounts for repulsive $A_{\alpha\beta}/r_{ij}^{12}$ and dispersive $-B_{\alpha\beta}/r_{ij}^{6}$ interactions, the parameters are listed elsewhere.[7]

In the molecular mechanics (MM) simulations, the time-consuming Ewald summation is not performed, the electrostatic and (L−J) interaction cutoffs are defined by two parameters: the spline-on and the spline-off distances. Within these ranges the nonbonded interaction energy is attenuated by the spline function. Beyond the spline-off distance, nonbonded interactions are ignored. The spline-on and spline-off distances are taken to be 1.5 and 3 nm for both the electrostatic and (L−J) interactions. The Si, Al, O, H atoms of the zeolite framework were taken to be fixed and the bpyH$_n^{+n}$ structure was taken to be mobile and flexible. The energy term is reduced to $E = E_S + E_{ZS}$ and the energy minimization of E is performed using the conjugate gradient minimization procedure.

Results and Discussion

Protonation of 4,4′- and 2,2′-Bipyridine in Aqueous Media. The protonated form of pyridine PyH$^+$ has a dissociation constant of 5.25 (pK_a). The diprotonated form, 4,4′-bpyH$_2^{2+}$ in which two pyridinium rings are bound with 4,4′-carbon atoms possesses lower constants than pyridinium, 2.5 (pK_{a1}) and 4.9 (pK_{a2}), respectively. The diprotonated form, 2,2′-bpyH$_2^{2+}$ in which two pyridinium rings are bound with 2,2′-carbon atoms exhibits much lower constant of −0.2 (pK_{a1}) while the second pK_{a2} is 4.4, weakly lower than that of 4,4′-bpyH$_2^{2+}$.[23]

The 4,4′-bpyH$_2^{2+}$ dication in 4,4′-bipyridinium nitrate exhibits a twisted structure with a dihedral angle value of 39.0°.[24] The optimized geometry of N,N′-diprotonated 4,4′-bpy species was recently calculated.[22,25] The resulting structure has twisted conformations with D_2 molecular symmetry group. To our knowledge, the published Raman data of protonation of 4,4′-bpy in acidic aqueous solution provide evidence of an intermediate species but no Raman spectrum of pure monoprotonated 4,4′-bpyH$^+$ species can be extracted to be compared with the calculated frequencies.[22,26] Because there was no evident direct implication of the monoprotonated 4,4′-bpyH$^+$ species in the protonation of 4,4′-bpy in acidic ZSM-5 zeolites (see below), no additional investigation in aqueous media was undertaken in the present work (Figure 1).

In the same way, the optimized geometries of N-monoprotonated 2,2′-bpyH$^+$ were calculated at ab initio level.[4]

Although many studies have been made on the UV absorption spectra and protonation constants of 2,2′-bpy, the conformations of the protonated forms in solution have not been reported yet.[27] As demonstrated in the following paragraphs, the implication of the 2,2′-bpyH$^+$ species in the sorption of 2,2′-bpy in acidic ZSM-5 zeolites has made the extensive study of the protonation of 2,2′-bpy in aqueous media by Raman spectroscopy inevitable. The FT-Raman spectra of 2,2′-bpy in aqueous solutions at pH ranging between 12 and −1.5 were recorded. The 31 spectra were treated using the SIMPLISMA procedure (see Experimental Section). This analysis yields four typical spectra, Figure 2. The reconstructed spectra obtained from the extracted spectra of individual species were found to be in agreement with the experimental spectra. Residuals are small and have a random pattern. Associated parameter was found to be RRSSQ = 0.018 (see Experimental Section).

The neutral *trans*-2,2′-bpy, Figure 2a was identified by direct comparison with previously reported spectra for pure 2,2′-bpy species in solution.[28] In solution, several previous experimental studies such as dipole moments provide concordant evidence for a planar or approximately *trans* planar conformation in all the solvents.[29,30] This species only appears at high pH values.

(23) Heyrovski, M.; Novothy, L. *Czech. Chem. Commun*. 1987, *52*, 54.
(24) Barker, D. J.; Buckleton, J. S.; Clark, G.; Cooney, R. P.; Rickard, C. E. *J. Mol. Struct*. **1990**, *239*, 249.
(25) Ould-Moussa, L.; Poizat, O.; Castella-Ventura, M.; Buntinx, G.; Kassab, E. *J. Phys. Chem.* **1996**, *100*, 6, 2072.
(26) Lu T.; Cotton T. M.; Birke R. L.; Lombardi J. R. *Langmuir* **1989**, *5*, 406.
(27) Nakamoto, K. *J. Phys. Chem*. **1960**, *64*, 1420.
(28) Ould-Moussa, L.; Castella-Ventura, M.; Kassab, E.; Poizat, O.; Strommen, D. P.;Kincaid, J. R. *J. Raman Spectrosc*. **2000**, *31*, 377.
(29) Cumper C. W. N.; Ginman R. F. A.; Vogel A. *J. Chem. Soc*. **1962**, 1188.
(30) Cureton P. H.; Le Fèvre C. G.; Le Fèvre R. J. W. *J. Chem Soc*. **1963**, 1736.

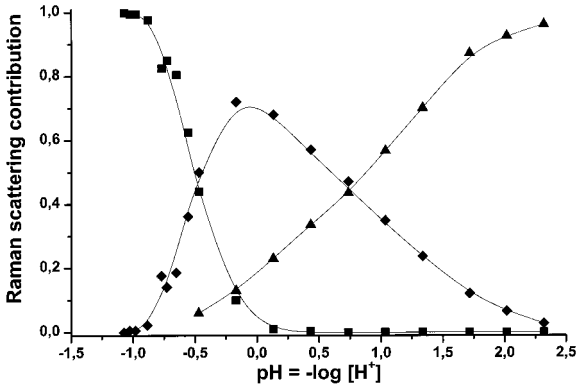

Figure 3. Relative contribution deduced from SIMPLISMA method of pure species to the Raman spectra as a function of pH = −log [H^+]: (▲) *trans*-2,2′-bpyH^+; (◆) *cis*-2,2′-bpyH^+; (■) 2,2′-bpyH_2^{2+}.

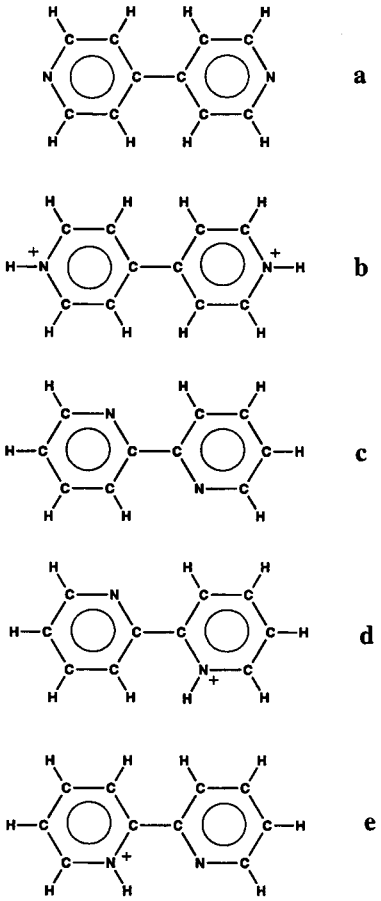

Figure 4. Schematic structures of: (a) 4,4′-bpy; (b) 4,4′-bpyH_2^{2+}; (c) *trans*-2,2′-bpy; (d) *trans*-2,2′-bpyH^+; (e) *cis*-2,2′-bpyH^+; (f) *trans*-2,2′-bpyH_2^{2+}.

At low pH values, two analogous but different spectra were extracted for the (*trans* and *cis*) diprotonated 2,2′-bpyH_2^{2+} species using the SIMPLISMA procedure. The spectrum corresponding to the major contribution is presented in Figure 2d. However, there was no evident direct implication of the diprotonated species in the protonation of 2,2′-bpy in acidic ZSM-5 zeolites (see below); therefore, no additional discussion was done in the present work.

The two remaining extracted spectra, Figure 2, b, c, were straightforwardly assigned to monoprotonated *trans*- and *cis*-2,2′-bpyH^+. The vibrational analysis of the extracted spectra of 2,2′-bpyH^+ points out two different behaviors of the two pyridine rings, the protonated and nonprotonated rings. Particularly, the bands with wavenumbers higher than 1600 cm^{-1} are characteristic of the protonated ring, while the sharp bands between 1550 and 1600 cm^{-1} are typical of the pyridine ring.

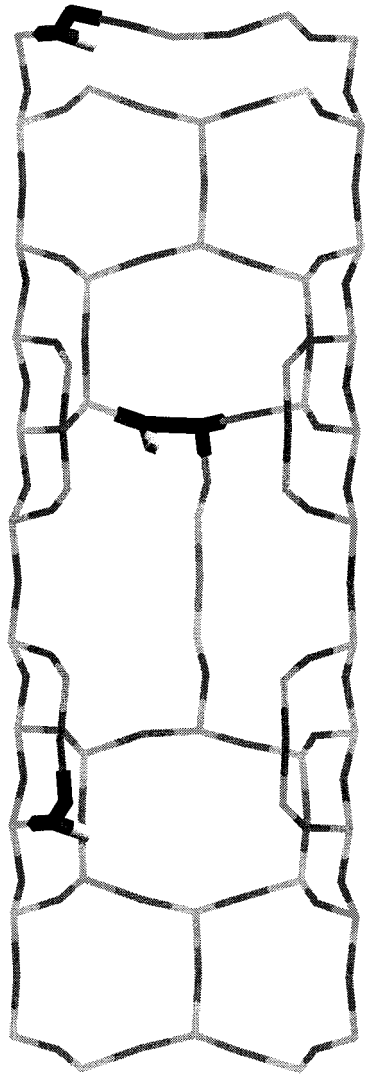

Figure 5. Straight channel (view in the b, c plane) of empty HZSM-5 zeolite. Black and shaded sticks represent the O and Si atoms of the framework, respectively. The white and black cylinders represent the H and Al atoms, respectively.

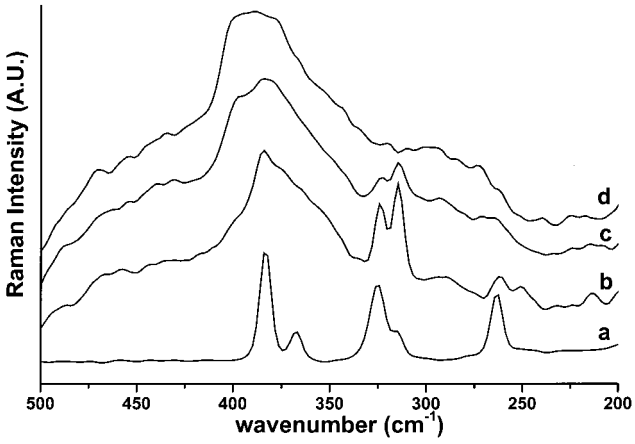

Figure 6. Sorption of 4,4′-bpy in H_6ZSM-5 monitored by FT-Raman spectrometry at room temperature in the low-frequency region (1 bpy/unit cell): (a) 4,4′-bpy in the solid state; (b) 1 day after the mixture of the powders; (c) 10 days; (d) 3 months.

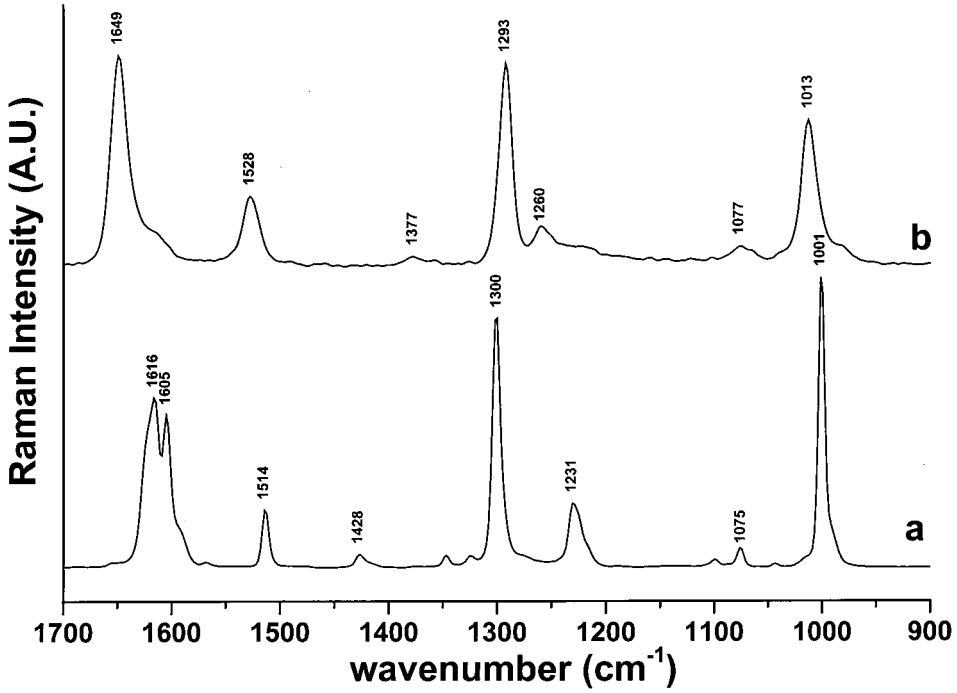

Figure 7. Pure Raman spectra extracted by the SIMPLISMA method of the FT-Raman data recorded during the sorption of 4,4′-bpy in H_nZSM-5 zeolites ($n = 3,6$): (a) solid 4,4′-bpy; (b) 4,4′-bpyH_2^{2+}.

In addition, the breathing mode of the protonated ring is observed at 1011 and 1013 cm^{-1}, whereas the corresponding mode of the neutral ring occurs at 997 and 999 cm^{-1}, respectively (Table 1). The expected molecular symmetry groups of the *cis* and *trans* conformers are C_s (planar) or C_1 (nonplanar), and there are no symmetry and vibrational arguments to assign the *cis* or *trans* conformation to the Raman spectra. The wavenumbers of the characteristic Raman bands are found to be analogous, except for a more intense band near 1650 cm^{-1} in the spectrum shown in Figure 2b. However, the relative intensities are more typical of the conformation changes, Figure 2.

Previous calculations at ab initio levels indicate the existence of a stable *cis*-2,2′-bpyH^+ with planar conformation (C_s), while the *trans* form has an interplanar angle of ∼26°. The *cis* conformer is by far the most stable.[4] The barrier to *trans/cis* (∼14 kJ·mol^{-1}) or *cis/trans* (∼43 kJ·mol^{-1}) interconversion is of central importance in understanding the basicity of 2,2′-bpy, since without it the *trans* protonated species would instantaneously interconvert to the much more stable *cis* form, giving rise to a much larger observed pK_a. It was demonstrated previously that the rotation from *trans* to *cis* conformation increases the power of acidity (PA) of the remaining aza group by about 40 kJ·mol^{-1}.[4] These theoretical considerations and the results of the present FT-Raman experiments lead to think that the 2,2′-bpyH^+ with *trans* conformation (Figure 2b) is preponderant around pH 2 whereas *cis*-2,2′-bpyH^+ (Figure 2c) around pH 0, Figure 3.

The relative Raman contribution of each pure species to the Raman scattering is deduced using the SIMPLISMA software (see Experimental Section). The relative contribution of each species to the Raman spectra can be represented as a function of pH = −log[H^+], Figure 3. The respective 2,2′-bpy and 2,2′-bpyH_2^{2+} contributions behave as expected from calculations using the pK_a values (−0.2 and 4.4). The main contributions of *trans*- or *cis*-2,2′-bpyH^+ occur between pH 2 and −0.5. In this pH range, the ratio of the two species depends on the pH values. However, the driving forces to the conformational change do not appear to be pH-dependent (Figure 4).[4]

Characterization of Calcined H_nZSM-5 Zeolites. The framework structure of ZSM-5 zeolites contains two types of intersecting channels, both formed by rings of 10 oxygen atoms, characterizing them as a medium-pore zeolite.[19−21] One channel type is straight and has a nearly circular opening (0.53 nm × 0.56 nm), while the other one is sinusoidal and has an elliptical opening (0.51 nm × 0.55 nm). These channels are sufficiently wide to permit bipyridine molecules to pass through these types of channels and to diffuse into the void space (Figure 5).

Brønsted acid sites (BAS) are assigned to bridging hydroxyl groups Al−OH−Si. Thus far, the problem of locating the Al atoms and associated proton or deuterium in H(D)-ZSM-5 by X-ray or neutron diffraction techniques failed. However, numerous theoretical and experimental investigations provide significant findings about the distribution, structure, and acid strength of Brønsted acid sites of H-ZSM-5 zeolites with analogous chemical contents as determined for the samples under study.[31,32] The chemical analysis, X-ray diffraction pattern, and ^{27}Al MAS NMR measurements do not provide evidence of any aluminum extraframework amount in $H_{3.0}(AlO_2)_{3.0}(SiO_2)_{93.0}$ and $H_{3.4}(AlO_2)_{3.4}(SiO_2)_{92.6}$ calcined samples. However, the sample with the following framework composition, $H_{6.6}(AlO_2)_{6.6}$-$(SiO_2)_{89.4}$, exhibits a significant amount of extraframework aluminum, represented as 0.3 Al_2O_3 per unit cell.

The Brønsted acid sites were characterized by FT-IR absorption spectra in the OH stretching region. In the spectra of all samples calcined at 773 K under Ar or O_2 a strong band at 3612 cm^{-1} (Si/Al = 27) or 3640 cm^{-1} (Si/Al = 13) due to the bridged OH was detected, while a low intensity band can be seen at about 3740 cm^{-1} which can be attributed to silanol group. It was previously demonstrated that the IR absorption in the OH stretching region decreases drastically after activation at higher temperature particularly under O_2.[33] To our knowledge, no structural determination concerning the aluminum and acid

(31) Grau-Crespo, R.; Peralda, A. G.; Ruiz-Salvador, A. R.; Gomez, A.; Lopez-Cordero, R. *Phys. Chem. Chem. Phys.* **2000**, *2*, 5716.

(32) Catana, G.; Baetens, D.; Mommaerts, T.; Schoonheydt, R. A.; Weckhuysen, B. M. *J. Phys. Chem. B* **2001**, *105*, 4904.

site distributions over the ZSM-5 crystals under study was made.[31] However, a previous work provides a clear picture of the distribution of acid sites in large ZSM-5 zeolite crystals.[34]

Numerous papers and reviews have been published about the Fourier transform infrared spectroscopy (FTIR) and probe molecules such as pyridine, ammonia and acetonitrile to study the acidity of zeolites.[13] In a recent paper, the Brønsted acid strength distribution of H-ZSM-5 zeolites with Si/Al $\approx$ 19−29 and activated at 800 K in air was estimated using temperature-programmed desorption of ammonia.[35]

It was demonstrated previously that the Lewis acidity of the H-ZSM-5 samples increases markedly as a function of the calcination temperature under O_2 between 600 and 1000 K, whereas the nonframework Al content has a weak effect on the Lewis acidity.[32] Lewis acid sites (LAS) are essentially electron-acceptor centers and they can be different aluminum species located in defect centers, the so-called true Lewis sites. The origins of Lewis acidity in zeolites are diverse and depend on the structure and chemical composition of the material under investigation. The structure of true Lewis sites is still contreversial. Some authors associate LAS with trigonal Al atoms formed as a result of zeolite dehydroxylation by thermal treatment. Other research groups have proposed Al^{3+} species or other various nonframework species (AlO^+, $Al(OH)^{2+}$, $Al(OH)_3$, $AlO(OH)$, Al_2O_3, etc.) leached from the zeolite framework during chemical or thermal treatment. The exact nature of these species is, however, still unknown.[32]

The calcined zeolite samples used for the following bipyridine sorption studies were found to exhibit Brønsted acidity sites and, to a lesser extent, Lewis acidity sites.

Sorption of 4,4′-Bipyridine in Acidic H_nZSM-5 Zeolites. Solid 4,4′-bpy exhibits vapor pressure that is too weak at room temperature to carry out the sorption procedure through sublimation from a compartment containing the solid 4,4′-bpy to another compartment containing the freshly H_nZSM-5 dehydrated zeolite samples even under gentle warming. The adsorption from bpy solution in organic solvent can be an alternative to avoid this problem. However, it is then difficult to eliminate the solvent from the void space without damaging the sample. The method used is mixing weighted amounts of dehydrated H_nZSM-5 ($n = 3, 6$) and dry pure 4,4′-bpy (1 or 2 mol/unit cell) in the same reactor under dry argon atmosphere. The cell was allowed to stand at room temperature for several weeks until the sorption of guest molecules into the void space of the zeolites went to completion. The sorption process at loading corresponding to 1 molecule per unit cell was monitored as a function of time by FT-Raman and UV−visible absorption spectrometry. The two techniques provide coherent clues; however, the Raman spectrometry was found to lead to more pertinent structural results.

Progressively over several weeks, the spectral features in mid- and low-frequency regions evolved from the spectrum characteristics of bulk state to the spectrum relative to the occluded species. Low-frequency Raman spectra provide an interesting way to estimate the sorption course through the dramatic intensity decrease of the characteristic bands of 4,4′-bpy bulk state at 265, 315, 325, and 385 cm^{-1}, whereas the low-frequency Raman bands assigned to the deformation modes of the host framework around 300−380 cm^{-1} do not change markedly upon sorption (Figure 6).

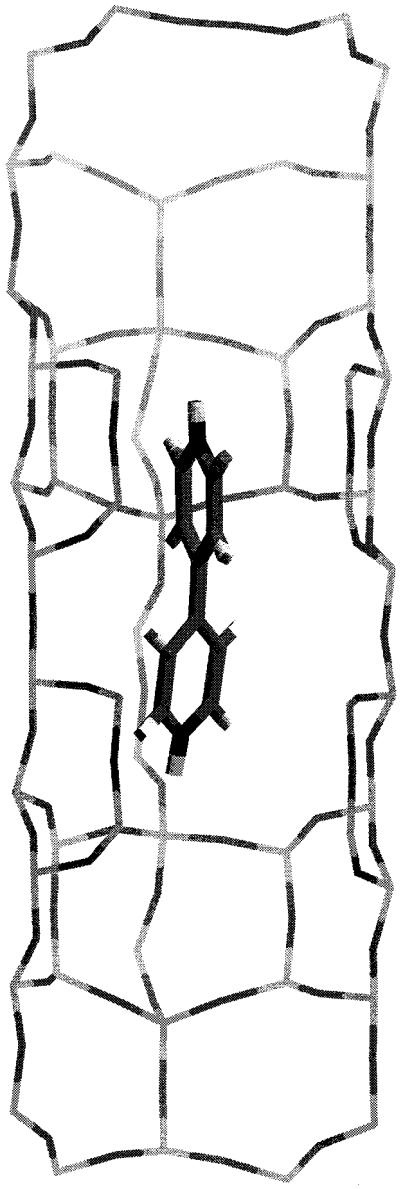

Figure 8. Expected conformation and sorption site of 4,4′-bpyH_2^{2+} occluded in straight channel *(view in the b, c plane)* of HZSM-5 zeolite. Black and shaded sticks represent the O and Si atoms of the framework, respectively. The white, shaded, and black cylinders represent the H, C and N atoms of 4,4′-bpyH_2^{2+}, respectively.

The data processing using the SIMPLISMA approach of all the spectra recorded in the mid-frequency region during the course of the sorption in H_nZSM-5 samples provides evidence of two independent spectra for each attempt and all the attempts. The reconstructed spectra obtained from the extracted spectra of individual species were found to be in agreement with the experimental spectra. Residuals are small and have a random pattern. The associated parameter was found to be RRSSQ less than 0.02 (see Experimental Section).

The remaining 4,4′-bpy solid was straightforwardly identified through the FT-Raman spectrum, while the assignment of spectra corresponding to the occluded species needed careful comparison with all the available Raman spectra concerning neutral and protonated species concerning 4,4′-bpy.[26]

The Raman spectra of the occluded species (Figure 7) and 4,4′-bpyH_2^+ in acidic aqueous solution (Figure 1) are found to be identical in wavenumber as well as in relative intensities. 4,4′-bpyH_2^+ appears as the unique species in the void space of

(33) Smirnov, K. S.; Tsyganenko. A. A. *Chem. Phys. Lett.* **1991**, *182*, 127.
(34) Schüth, F.; Althoff, R. *J. Catal.* **1993**, *143*, 388.
(35) Costa C.; Dzikl, I. P.; Lopes, J. M.; Lemos, F.; Ribeiro, F. R. *J. Mol. Catal. A* **2000**, *154*, 193.

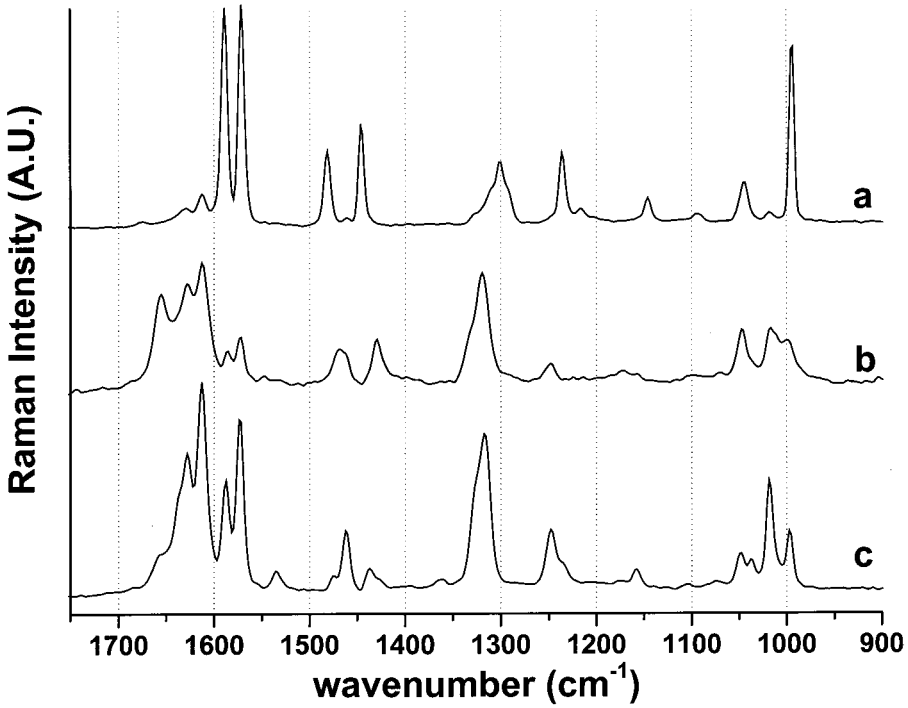

Figure 9. Pure Raman spectra extracted by the SIMPLISMA method of the FT-Raman data recorded during the sorption of 2,2′-bpy in H_nZSM-5 zeolites ($n = 3,6$): (a) solid 2,2′-bpy; (b) *trans*-2,2′-bpyH$^+$; (c) *cis*-2,2′-bpyH$^+$.

the H_nZSM-5 zeolites under study at loading, corresponding to one or two 4,4′-bpy per unit cell. The comparison between the spectra previously reported for 4,4′-bpy occluded in Na_nZSM-5, silicalite-1 and the present spectrum indicates no analogy. The observation of additional Raman bands around 3110 cm^{-1} and assigned to the N−H stretching mode validates the N protonation of the 4,4′-bpy within the void space.[22] The proton transfer occurs from the bridging hydroxyl groups Al−OH−Si of the framework to the N and N′ atoms of the 4,4′-bipyridine as observed in HCl aqueous solutions at pH less than 2. The strict analogy between the observed and the calculated frequencies[22,25] permits the attribution of a twisted conformation to the occluded N,N′-diprotonated cation. Furthermore, the analogy in wavenumber and relative intensity between the HCl/H_2O solution and occluded 4,4′-bpyH_2^{2+} spectra demonstrates that the motions of 4,4′-bpyH_2^{2+} within the channel of ZSM-5 are in the range of the isotropic limit of a liquid at room temperature.

No additional Raman band corresponding to possible 4,4-bpy interacting with Lewis sites of the host was detected. In contrast, Lewis and Brønsted acid sites are distinguished in IR absorption spectra of pyridine sorbed in H-ZSM-5 with analogous aluminum content and calcination procedure.

The energy minimization was carried out with a rigid twisted conformation of 4,4′-bpyH_2^{2+}.[25] The calculations provide a reasonable structural picture of the 4,4′-bpyH_2^{2+} moiety occluded in ZSM-5, Figure 8. The dication was found to be located in a straight channel in the vicinity of the intersection with the zigzag channel and the central C−C bond runs along the b direction. The sorption site and conformation of 4,4′-bpyH_2^{2+} in the void space of H_nZSM-5 appear to be analogous to those previously reported for neutral 4,4′-bpy occluded in Na_nZSM-5 or in silicalite.[8] The sorption of 4,4′-bpy goes to completion over 3 months at room temperature, and the sorption and the protonation of 4,4′-bpy appear simultaneous from the beginning to the end of the sorption. The sorption rate was found to be in the same order as that recently reported for neutral 4,4′-bpy sorption in Na_nZSM-5 or in silicalite. Nevertheless, the 4,4′-bpy sorption rate was found to be dramatically slower than that of pyridine in H_nZSM-5 zeolites.[13]

Sorption of 2, 2′-Bipyridine in Acidic H_nZSM-5 Zeolites. FT-Raman spectra were recorded at room temperature after the mixing and shaking of dry solid 2,2′-bpy (1 or 2 mol/unit cell) with calcined H_nZSM-5 ($n = 3, 6$) powdered samples. Progressively, over several weeks, the spectral features in mid and low-frequency regions evolved from the spectrum characteristics of bulk state to spectra relative to occluded species. Low-frequency Raman spectra provide an interesting way to estimate the sorption course through the progressive intensity decrease of the characteristic bands of 2,2′-bpy bulk state particularly at 224, 332, and 439 cm^{-1}.

The data processing using the SIMPLISMA approach of all the spectra recorded in the mid-frequency region during the course of the sorption in H_nZSM-5 samples provide evidence of two or three independent spectra for each attempt and three for all the attempts. The reconstructed spectra obtained from the extracted spectra of individual species were found to be in agreement with the experimental spectra. Residuals are small and have a random pattern. Associated parameter (RRSSQ) was found to be less than 0.04 (see Experimental Section).

The remaining 2,2′-bpy solid was straightforwardly identified through the FT-Raman spectrum, while the assignment of spectra corresponding to the occluded species were made through careful comparison with the Raman spectra of the protonated species determined in acidic aqueous media, Figures 2 and 9.

According to the significant similarities between the Raman spectra of 2,2′-bpy occluded in H_nZSM5 and dissolved in HCl aqueous solutions, it is clear that the sorption of 2,2′-bpy in acidic ZSM-5 leads to complete N-monoprotonation of the sorbate as *cis*- and *trans*-2,2′-bpyH$^+$ for all the zeolites used ($n = 3,6$) and for all the loading values (1 or 2 mol/unit cell, Table 1). Protonation process is confirmed by the observation of N−H stretching modes at ca. 3110 cm^{-1}. The proton transfer occurs from the bridging hydroxyl groups Al−OH−Si of the zeolite framework to one N atom of 2,2′-bpy as observed in HCl

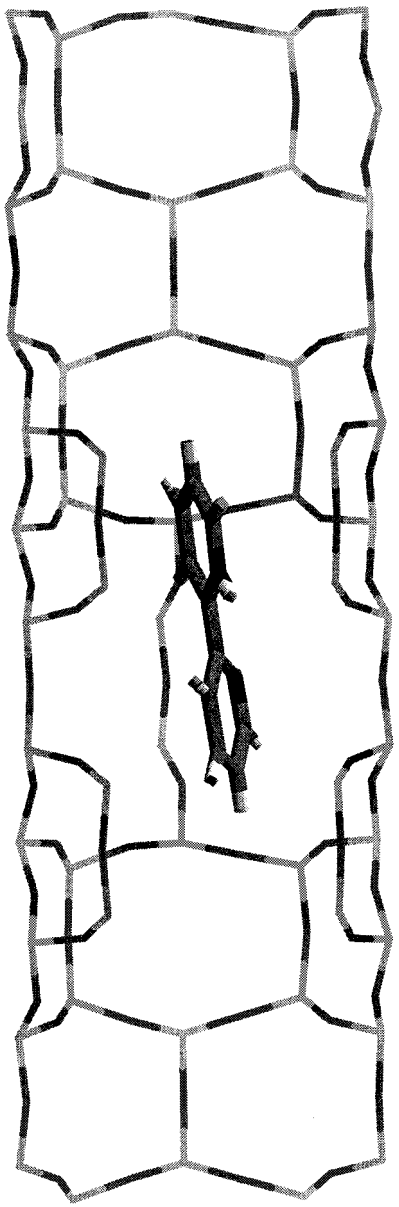

Figure 10. Expected conformation and sorption site of *trans*-2,2′-bpyH$^+$ occluded in straight channel *(view in the b, c plane)* of HZSM-5 zeolite. Black and shaded sticks represent the O and Si atoms of the framework, respectively. The white, shaded, and black cylinders represent the H, C, and N atoms of 2,2′-bpyH$^+$, respectively.

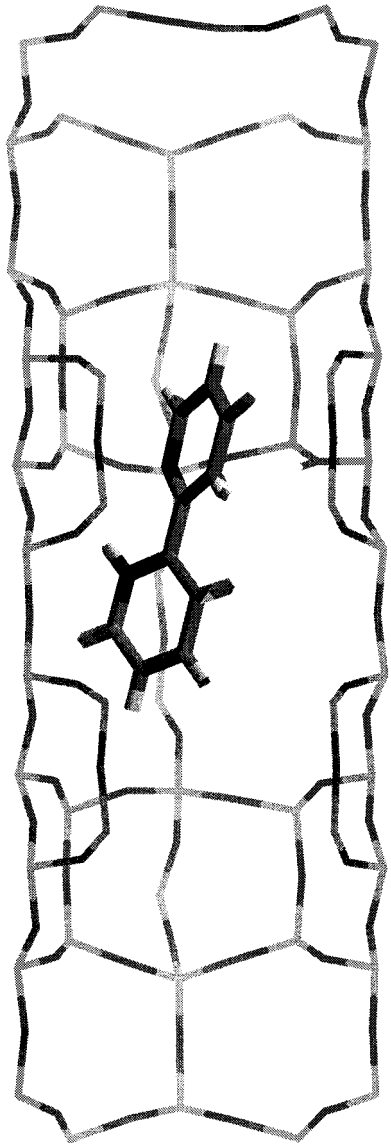

Figure 11. Expected conformation and sorption site of *cis*-2,2′-bpyH$^+$ occluded in straight channel *(view in the b, c plane)* of HZSM-5 zeolite. Black and shaded sticks represent the O and Si atoms of the framework, respectively. The white, shaded, and black cylinders represent the H, C, and N atoms of 2,2′-bpyH$^+$, respectively.

aqueous solutions at pH less than +2 but more than −0.3. The analogy between the frequencies and relative intensities of the corresponding Raman bands assigned to *cis*- and *trans*-2,2′-bpyH$^+$ in aqueous solutions and occluded in ZSM-5 permits the attribution of conformations as deduced from previous calculations at ab initio level.[4] Nevertheless, some differences observed in the wavenumbers and relative intensities as well as in the bandwidths between some corresponding Raman bands indicate the motions of 2,2′-bpyH$^+$ within the channel of ZSM-5 are hindered but remain in the range of the isotropic limit of a liquid at room temperature. It should be noted that the Raman band assigned to the breathing mode of the protonated pyridyl ring for the *cis* mono protonated conformation shifts from 1018 to 1011 cm^{-1} from the void space of ZSM-5 to the aqueous solution, respectively.

The energy minimization was performed with rigid twisted conformations of *cis*- and *trans*-2,2′-bpyH$^+$ cations. The calculations provide reasonable structural pictures of cations occluded in ZSM-5, Figures 10, 11. The cations were found to be located in straight channels in the vicinity of the intersection with the zigzag channel, and the central C−C bond runs along the *b* direction.

H_nZSM-5 zeolites uptake 2,2′-bpy over 2 months at room temperature, and the sorption and the N-protonation of 2,2′-bpy are found to be simultaneous from the beginning to the end of the sorption. The sorption rate was found to be in the same order as that obtained for 4,4′-bpy sorption. The sorption of 2,2′-bpy in H_nZSM-5 ($n = 3, 6$) at loadings corresponding to 1 mol per unit cell leads to *trans*-N-protonated 2,2′-bpyH$^+$ as major species, Figure 12, whereas the sorption at loading corresponding to 2 mol per unit cell generates both *trans*- and *cis*-2,2′-bpyH$^+$, Figure 13. It should be noted that *trans/cis* interconversion occurs even after the complete uptake of the sorbate, and indicates some rearrangement in the void space over a long time at high loading. The acidity does not appear to be the main driving force to the conformation change and has to be combined with the confinement effects within the

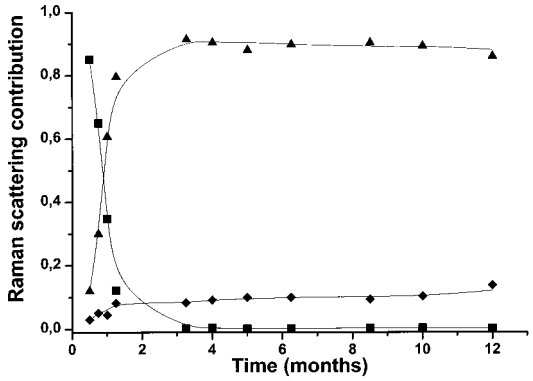

Figure 12. Relative contribution deduced from SIMPLISMA method of pure species to the Raman spectra as a function of sorption time at one 2,2′-bpy/H_6ZSM-5: (▲) *trans*-2,2′-bpyH$^+$; (◆) *cis*-2,2′-bpyH$^+$; (■) solid 2,2′-bpy.

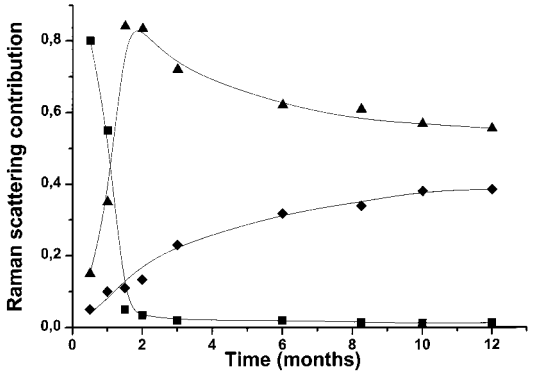

Figure 13. Relative contribution deduced from SIMPLISMA method of pure species to the Raman spectra as a function of sorption time at two 2,2′-bpy/H_6ZSM-5: (▲) *trans*-2,2′-bpyH$^+$; (◆) *cis*-2,2′-bpyH$^+$; (■) solid 2,2′-bpy.

available void space. The electrostatic and steric effects on such a small *trans/cis* barrier is large enough to observe measurable populations of the *cis* cation at room temperature, and of course, this equilibrium could be further shifted toward the *cis* cation in the presence of an appropriate environment.

Conclusions

The data processing of the Raman spectra recorded during the protonation of 2,2′- or 4,4′-bpy in hydrochloric aqueous solutions provide specific Raman spectrum of each protonated species generated in acidic aqueous media as well as their respective contributions to the Raman scattering as a function of the [H$^+$] concentration. All the contributions of neutral and cationic species were found to be in agreement with the expected concentrations calculated through the pK_a values. However two species with analogous Raman spectra were found to correspond to the 2,2′-bpyH$^+$ cation. These species assigned to *cis* and *trans* conformations were expected from theoretical calculations. Previous calculations at semiempirical and ab initio levels indicate the existence of *cis*- and *trans*-2,2′-bpyH$^+$ forms. The *cis* conformer is by far the most stable. The barrier to *trans/cis* interconversion is of central importance in understanding the basicity of 2,2′-bpy, since without it the *trans* protonated species would instantaneously interconvert to the much more stable *cis* form, giving rise to a much larger pK_a.

The data processing of the Raman spectra recorded during the slow sorption of 4,4′-bpy in acidic H_nZSM-5 (n = 3, 6) zeolites provide specific Raman spectrum of N,N′-diprotonated dication 4,4′-bpyH_2^{2+} as unique species generated in the void space of acidic ZSM-5 zeolites. In contrast with pyridine sorption monitored by FTIR absorption spectroscopy, no evidence of Lewis acid sites was found during the sorption of 4,4′-bpy by Raman scattering spectroscopy.

The data processing of the Raman spectra recorded during the slow sorption of 2,2′-bpy in acidic H_nZSM-5 (n = 3, 6) zeolites provide specific Raman spectrum of *trans*-N-monoprotonated cation 2,2′-bpyH$^+$ as species generated in the void space of acidic ZSM-5 zeolites at loading corresponding to 1 mol per unit cell. The *trans/cis* interconversion occurs at higher loading even after the complete uptake of the sorbate and indicates some rearrangement in the void space over a long time. The electrostatic and steric effects on such a small *trans/cis* barrier is large enough to observe measurable populations of the *cis* cation at room temperature, and this equilibrium could be further shifted toward the *cis* cation in the presence of an appropriate environment. The cations were found to be located in straight channels in the vicinity of the intersection with the zigzag channel with the expected conformation. However, the motions of 2,2′-bpyH$^+$ within the channel of ZSM-5 are hindered but remain in the range of the isotropic limit of a liquid at room temperature.

Acknowledgment. We are very grateful to Dr. B. Sombret for his assistance and advice while using FT-Raman spectrometer. We acknowledge Dr. J. Patarin for helpful discussions and advice. The Centre d'Etudes et de Recherches Lasers et Applications (CERLA) is supported by the Ministère chargé de la recherche, the région Nord/Pas de Calais, and the Fonds Européen de Développement Economique des Régions.

JA011787B